

Double peaks of gravitational wave spectrum induced from inflection point inflation

Tie-Jun Gao^{1*} and Xiu-Yi Yang²

¹*School of Physics and Optoelectronic Engineering,*

Xidian University, Xi'an 710071, China

²*School of science, University of Science and Technology Liaoning, Anshan 114051, China*

Abstract

We investigate the possibility to induce double peaks of gravitational wave spectrum from primordial scalar perturbations in inflationary models with three inflection points. Where the inflection points can be generated from a polynomial potential or generated from Higgs like ϕ^4 potential with the running of quartic coupling. In such models, the inflection point at large scales predicts the scalar spectral index and tensor-to-scalar ratio consistent with current CMB constraints, and the other two inflection points generate two large peaks in the scalar power spectrum at small scales, which can induce gravitational waves with double peaks energy spectrum. We calculate the induced gravitational wave energy spectrum and find that the double peaks signal can be detected in near future and can be distinguished with other single peak models.

Keywords: inflation, gravitational waves, inflection point

* tjgao@xidian.edu.cn

I. INTRODUCTION

Gravitational wave(GW) astronomy is began since the detection of GWs produced by the merging of black holes or neutron stars by the LIGO and Virgo collaborations [1–6]. Besides these GWs from mergers, the GWs can also be generated from perturbation theory of inflation, so it becomes important to study inflationary theories using GWs as probes. The current constraint of the tensor-to-scalar ratio on CMB scales is $r < 0.064$ at 95% confidence level [7] by the Planck 2018 data in combination with BICEP2/Keck Array, which is too small to be detected in the near future.

Although at first order in perturbation theory the scalar and tensor perturbations are decoupled, however, at second order they are coupled, so the second-order GWs can be induced from scalar perturbations when it reenter the Hubble radius in the radiation-dominated(RD) era [8, 9]. In most of the inflationary models, the induced second-order GWs is generically negligible compared to first-order GWs. However, if the power spectrum of scalar perturbations is enhanced at small scales, the second-order GWs can be sizable or even larger than the first-order one [10–17].

One way to realize the enhancement of the power spectrum at small scales in single field inflation is using an inflection point [18–22]. The inflection point is such point that both the first and second derivatives of the potential vanish. Near the inflection point the Hubble slow-roll parameter $|\eta_H| > 3$, so the slow-roll approximation fails and the ultra-slow-roll trajectory supersedes, which gives rise to a large peak in the scalar power spectrum at small scales, and generate induced GWs with a peak in the energy spectrum. Such inflection point can be generated from critical Higgs inflation [23, 24], supergravity [25, 26], string theory [27–30] etc.

The previous models with single inflection point only lead to one peak in the scalar power spectrum, with the width about 20 e-folding numbers. As we all know that the e-folding numbers during inflation is about 50–60, so it seems possible to generate a power spectrum with two peaks using inflection points. Thus in this paper, we shall investigate the possibility to induce GW spectrum with double peaks by the scalar power spectrum which have two peaks at small scale. We show that such kinds of power spectrum can be generated from the

potential with three inflection points, which is realized in a model with polynomial potential or in Higgs like ϕ^4 potential with the running of quartic coupling by radiative corrections. We calculate the GW energy spectrum, and imply that the double peak GW signal can be detected by SKA, LISA and other detectors in the near future, and can be distinguish with other single peak models.

The paper is organized as follows. In the next section, we brief review the mechanism of the GWs induced by first-order scalar perturbations. Then in Sec.3, we setup two inflationary models with three inflection points which can induce GWs with double peaks spectrum. The numerically results of the inflaton dynamics and the induced GWs in the two models are in Sec.4. The last section is devoted to summary.

II. GRAVITATIONAL WAVES INDUCED BY SCALAR PERTURBATIONS

In this section, we shall brief review the computation of induced GWs, for more details in Ref.[31–36]. In the conformal Newtonian gauge, the perturbed metric is written as

$$ds^2 = -a^2(1 + 2\Psi)d\eta^2 + a^2 \left[(1 - 2\Psi)\delta_{ij} + \frac{1}{2}h_{ij} \right] dx^i dx^j, \quad (1)$$

where Ψ is the scalar perturbations, and the Fourier components of tensor perturbations h_{ij} are defined as usual by

$$h_{ij}(\eta, \mathbf{x}) = \int \frac{d^3\mathbf{k}}{(2\pi)^{3/2}} e^{i\mathbf{k}\cdot\mathbf{x}} [h_{\mathbf{k}}^+(\eta)e_{ij}^+(\mathbf{k}) + h_{\mathbf{k}}^\times(\eta)e_{ij}^\times(\mathbf{k})], \quad (2)$$

where the two polarization tensors are

$$\begin{aligned} e_{ij}^{(+)}(\mathbf{k}) &= \frac{1}{\sqrt{2}} [e_i(\mathbf{k})e_j(\mathbf{k}) - \bar{e}_i(\mathbf{k})\bar{e}_j(\mathbf{k})], \\ e_{ij}^{(\times)}(\mathbf{k}) &= \frac{1}{\sqrt{2}} [e_i(\mathbf{k})\bar{e}_j(\mathbf{k}) + \bar{e}_i(\mathbf{k})e_j(\mathbf{k})], \end{aligned} \quad (3)$$

with the basis vectors $e_i(\mathbf{k})$ and $\bar{e}_i(\mathbf{k})$ orthogonal to each other and to \mathbf{k} . In the following, we shall omit the polarization index for simplicity.

In the Fourier space, the equation of motion of tensor modes can be derives from the Einstein equation as

$$h_{\mathbf{k}}''(\eta) + 2\mathcal{H}h_{\mathbf{k}}'(\eta) + k^2h_{\mathbf{k}}(\eta) = S_{\mathbf{k}}(\eta), \quad (4)$$

where $S_{\mathbf{k}}(\eta)$ is the Fourier transformation of the source term,

$$S_{\mathbf{k}}(\eta) = 4 \int \frac{d^3 p}{(2\pi)^{3/2}} e_{ij}(\mathbf{k}) p_i p_j \left(2\Psi_{\mathbf{p}} \Psi_{\mathbf{k}-\mathbf{p}} + \frac{4}{3(1+w)\mathcal{H}^2} (\Psi'_{\mathbf{p}} + \mathcal{H}\Psi_{\mathbf{p}}) (\Psi'_{\mathbf{k}-\mathbf{p}} + \mathcal{H}\Psi_{\mathbf{k}-\mathbf{p}}) \right). \quad (5)$$

The scalar perturbations $\Psi_{\mathbf{k}}$ can be split into the primordial value $\psi_{\mathbf{k}}$ and the transfer function $\Psi(k\eta)$

$$\Psi_{\mathbf{k}} \equiv \Psi(k\eta)\psi_{\mathbf{k}}. \quad (6)$$

If the peak mode enters the horizon in the RD era, the equation of state is $\omega = 1/3$, and then the transfer function becomes

$$\Psi(x) = \frac{9}{x^2} \left(\frac{\sin(x/\sqrt{3})}{x/\sqrt{3}} - \cos(x/\sqrt{3}) \right). \quad (7)$$

For the modes well inside the horizon, the density parameter of the GWs within the logarithmic interval of the wave numbers can be expressed in terms of the power spectrum of GWs

$$\Omega_{\text{GW}}(\eta, k) \equiv \frac{1}{\rho_c} \frac{d\rho_{\text{GW}}}{d \ln k} = \frac{1}{24} \left(\frac{k}{\mathcal{H}} \right)^2 \overline{\mathcal{P}_h(\eta, k)}, \quad (8)$$

with ρ_c is the critical energy density of the Universe, the overline denotes the oscillation average and the two polarization modes are summed up. The power spectrum $\mathcal{P}_h(\eta, k)$ is defined as

$$\langle h_{\mathbf{k}}(\eta) h_{\mathbf{p}}(\eta) \rangle = \frac{2\pi^2}{k^3} \delta^3(\mathbf{k} + \mathbf{p}) \mathcal{P}_h(\eta, k). \quad (9)$$

Using the Green's function method, the solution to the equation of $h_{\mathbf{k}}$ is

$$h_{\mathbf{k}}(\eta) = \frac{1}{a(\eta)} \int^\eta d\bar{\eta} G_{\mathbf{k}}(\eta, \bar{\eta}) a(\bar{\eta}) S_{\mathbf{k}}(\bar{\eta}), \quad (10)$$

where the Green's function $G_{\mathbf{k}}(\eta, \bar{\eta})$ satisfies

$$G''_{\mathbf{k}}(\eta, \bar{\eta}) + \left(k^2 - \frac{a''(\eta)}{a(\eta)} \right) G_{\mathbf{k}}(\eta, \bar{\eta}) = \delta(\eta - \bar{\eta}), \quad (11)$$

with the primes denote derivatives with respect to η . In the RD era, which is

$$G_{\mathbf{k}}(\eta, \bar{\eta}) = \frac{1}{k} \sin(k\eta - k\bar{\eta}). \quad (12)$$

Assuming $\psi_{\mathbf{k}}$ is Gaussian, the four-point correlation function of $\psi_{\mathbf{k}}$ can be transformed into the two-point correlation function. Then we obtain the power spectrum by introducing three dimensionless variables $u \equiv |\mathbf{k} - \mathbf{p}|/k$, $v \equiv |\mathbf{p}|/k$ and $x \equiv k\eta$, [13]

$$\mathcal{P}_h(\eta, k) = 4 \int_0^\infty dv \int_{|1-v|}^{1+v} du \left(\frac{4v^2 - (1 + v^2 - u^2)^2}{4uv} \right)^2 \mathcal{I}^2(x, u, v) \mathcal{P}_{\mathcal{R}}(ku) \mathcal{P}_{\mathcal{R}}(kv). \quad (13)$$

Consider the late-time limit $x \rightarrow \infty$, the term $\mathcal{I}(x, u, v)$ in the RD era can be calculated as

$$\begin{aligned} \mathcal{I}_{RD}(x \rightarrow \infty, u, v) = \frac{3(u^2 + v^2 - 3)}{4u^3v^3x} \left\{ \sin x \left[-4uv + (u^2 + v^2 - 3) \log \left| \frac{3 - (u+v)^2}{3 - (u-v)^2} \right| \right] \right. \\ \left. - \pi (u^2 + v^2 - 3) \Theta(v + u - \sqrt{3}) \cos x \right\}. \end{aligned} \quad (14)$$

After taking the oscillation average, one can obtain

$$\begin{aligned} \overline{\mathcal{I}_{RD}^2}(x \rightarrow \infty, u, v) = \frac{1}{2} \left(\frac{3}{4u^3v^3} \right)^2 (u^2 + v^2 - 3)^2 \\ \left\{ \left[-4uv + (u^2 + v^2 - 3) \ln \left| \frac{3 - (u+v)^2}{3 - (u-v)^2} \right| \right]^2 + \left[\pi (u^2 + v^2 - 3) \Theta(u + v - \sqrt{3}) \right]^2 \right\} \end{aligned} \quad (15)$$

Together with Eq. (8) and Eq. (13), and using $\mathcal{H} = 1/\eta$ in the radiation-dominated era, we finally get the energy spectrum of GWs

$$\begin{aligned} \Omega_{\text{GW}}(\eta, k) = \frac{1}{12} \int_0^\infty dv \int_{|1-v|}^{1+v} du \left(\frac{4v^2 - (1 + v^2 - u^2)^2}{4uv} \right)^2 \mathcal{P}_{\mathcal{R}}(ku) \mathcal{P}_{\mathcal{R}}(kv) \\ \left(\frac{3}{4u^3v^3} \right)^2 (u^2 + v^2 - 3)^2 \\ \left\{ \left[-4uv + (u^2 + v^2 - 3) \ln \left| \frac{3 - (u+v)^2}{3 - (u-v)^2} \right| \right]^2 + \left[\pi (u^2 + v^2 - 3) \Theta(u + v - \sqrt{3}) \right]^2 \right\} \end{aligned} \quad (16)$$

III. THE MODELS

A. Model I: A polynomial potential with inflection points

Motivated by an effective field theory with a cutoff scale Λ , a polynomial potential can be generally given by [37–42]

$$V_{\text{eff}}(\phi) = \sum_{n=0} \frac{b_n}{n!} \left(\frac{\phi}{\Lambda} \right)^n. \quad (17)$$

In principle, the effective potential contains higher order terms, however, since the inflection point is such point that both the first and second derivatives of V vanish, so in order to build a model with three inflection points, there must be six free parameters in the potential. Thus we truncate it to the eight-order here, and ignore the constant term and first order term to make the potential and its first-order derivative to be vanish at the origin. Then the potential can be parameterized as

$$V_{\text{eff}}(\phi) = V_0 \left[\frac{c_2}{2!} \left(\frac{\phi}{\Lambda} \right)^2 + \frac{c_3}{3!} \left(\frac{\phi}{\Lambda} \right)^3 + \frac{c_4}{4!} \left(\frac{\phi}{\Lambda} \right)^4 + \frac{c_5}{5!} \left(\frac{\phi}{\Lambda} \right)^5 + \frac{c_6}{6!} \left(\frac{\phi}{\Lambda} \right)^6 + \frac{c_7}{7!} \left(\frac{\phi}{\Lambda} \right)^7 + \frac{1}{8!} \left(\frac{\phi}{\Lambda} \right)^8 \right], \quad (18)$$

where V_0 is an overall factor, which can be constrained by the amplitude of scalar perturbations A_s , and c_{2-7} are six free parameters.

In some choices of parameter space, such potential allows the existence of inflection points, however it is non-renormalizable. So here we introduce an appropriate factor then the potential becomes

$$V(\phi) = \frac{V_{\text{eff}}(\phi)}{(1 + \xi\phi^2)^2}. \quad (19)$$

Such factor is usually arise from the scalar field non-minimal coupling to gravity[37, 42]. In some choices of parameter space, the potential $V(\phi)$ can generate three inflection points which can give an approximately scale invariant spectrum at large scales and make the prediction in good agreement with the current CMB measurements and at the same time generate two large peaks in the power spectrum at small scales to induce double peaks of GW spectrum.

For the convenience of discussion, we assume that the potential have three inflection point at ϕ_1, ϕ_2 and ϕ_3 , respectively, with $V'(\phi_i) = 0$ and $V''(\phi_i) = 0$. More general, in order to study slight deviations from a perfect inflection point, we introduce three more free parameters α_i and set $V'(\phi_i) = \alpha_i$ and $V''(\phi_i) = 0$. Then the parameters c_{2-7} in Eq.(18) can be expressed as functions of ϕ_i and α_i . By tuning the parameters, one can get a potential with three inflection points, which can both agree with the CMB constraints and induce a second-order gravitational waves spectrum with double peaks. For instance we take the

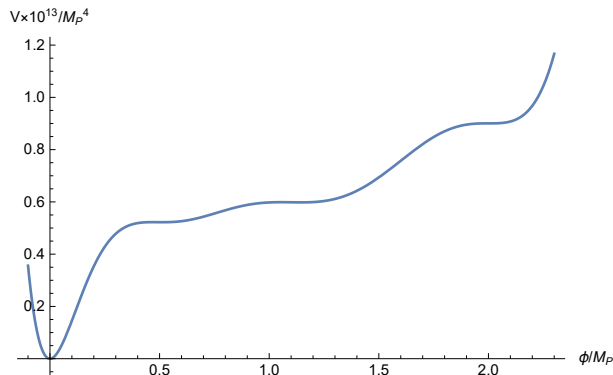


FIG. 1: Scalar potential $V(\phi)$ of model I for the parameters set (20).

following parameters set

$$\begin{aligned}
 V_0 &= 7.26 \times 10^{-11}, & \Lambda &= 0.5, & \xi &= 0.4, \\
 \phi_1 &= 0.49, & \alpha_1 &= -1.032325 \times 10^{-5}, \\
 \phi_2 &= 1.1, & \alpha_2 &= -1.65619 \times 10^{-5}, \\
 \phi_3 &= 2, & \alpha_3 &= 7.4 \times 10^{-7},
 \end{aligned} \tag{20}$$

and the corresponding potential are show in Fig.1.

We can see that there are three inflection points. The inflation starts near the first inflection point at high scale and leads to a nearly scale-invariant spectrum, then slowly rolls down the smooth plateau-like regions with a nearly constant Hubble friction. Whenever the inflaton meets a cliff, it speeds up quickly, until it reaches the next inflection point plateau where Hubble friction rapidly slows it down again, such point leads to a phase of ultra-slow-roll last about 20 e-folding numbers, which can generates a large peak in the power spectrum. Then near the last inflection point, the inflaton also becomes ultra-slow-roll and generates the second peak of the power spectrum.

B. Model II: A Higgs like potential with the running of quartic coupling

In this subsection, we shall consider a Higgs-like potential. During inflation the field values is large, so only the quartic part of the potential matters. Although the ϕ^4 model is

ruled out by the CMB observations, however, if one consider the interactions of the inflaton with other fields, required for reheating, the situation will be changed[43]. The radiative corrections can be accounted for through the running of the quartic coupling, then the potential can be approximated as

$$V(\phi) = \frac{\lambda(\phi)}{4!}\phi^4 \quad (21)$$

where $\lambda(\phi)$ is an effective field-dependent coupling, it can be parameterized as[21, 43]

$$\lambda = \lambda_0 \left[1 + b_1 \ln \left(\frac{\phi^2}{\phi_0^2} \right) + b_2 \ln \left(\frac{\phi^2}{\phi_0^2} \right)^2 + b_3 \ln \left(\frac{\phi^2}{\phi_0^2} \right)^3 + b_4 \ln \left(\frac{\phi^2}{\phi_0^2} \right)^4 + b_5 \ln \left(\frac{\phi^2}{\phi_0^2} \right)^5 + b_6 \ln \left(\frac{\phi^2}{\phi_0^2} \right)^6 \right] \quad (22)$$

where the overall factor λ_0 can be constrained by the amplitude of scalar perturbations, and the logarithms comes from two-loop and higher order terms in the Coleman-Weinberg expansion[44]. In order to make the potential have three inflection points, we truncate it to six-order here.

Similar to the Model I, we assume that the potential have three inflection points at ϕ_1, ϕ_2 and ϕ_3 , respectively, and set $V'(\phi_i) = \beta_i$ and $V''(\phi_i) = 0$ to study the slight deviations from a perfect inflection point. Then the six parameters $b_{1\sim 6}$ in Eq.(22) can be expressed as functions of ϕ_i and β_i . In some choices of parameter space, the potential $V(\phi)$ can also generate three inflection points which both in good agreement with the current CMB measurements and induce GWs energy spectrum with double peaks . For instance we take the following parameter set

$$\begin{aligned} \lambda_0 &= 1.124 \times 10^{-13}, & \phi_0 &= 1.57353, \\ \phi_1 &= 0.48, & \beta_1 &= -0.023885, \\ \phi_2 &= 1.1, & \beta_2 &= -0.14501, \\ \phi_3 &= 2, & \beta_3 &= 0.003, \end{aligned} \quad (23)$$

and the corresponding potential are show in Fig.2.

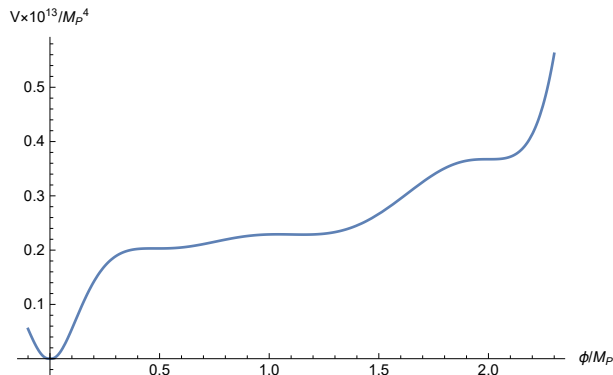


FIG. 2: Scalar potential $V(\phi)$ of Model II for the parameter set (23).

IV. NUMERICAL RESULTS

In this section, we shall numerically calculate the power spectrum of scalar perturbations and the energy spectrum of induced GWs in the Model I with parameter set (20) and in Model II with parameter set(23), respectively, then compare the results of $\Omega_{\text{GW},0}$ to the expected sensitivity curves of several planned GW detectors.

A. Inflaton dynamics

It has been pointed out in several references that near the inflection point the potential becomes extremely flat, thus the slow-roll approximation fails and is superseded by the ultra-slow-roll trajectory [45–48]. So one must use the Hubble slow-roll parameters instead the traditional one [49–51], which is defined as

$$\begin{aligned}\epsilon_H &= -\frac{\dot{H}}{H^2}, \\ \eta_H &= -\frac{\ddot{H}}{2H\dot{H}} = \epsilon_H - \frac{1}{2} \frac{d \ln \epsilon_H}{dN_e},\end{aligned}\tag{24}$$

with dots represent derivatives with respect to cosmic time, and N_e denote the e -folding numbers. In Fig.3, we plot the Hubble slow-roll parameters ϵ_H and η_H as functions of N_e for the two models, respectively. We can see that near the inflection points the Hubble slow-roll parameter $|\eta_H| > 3$, so the inflation becomes ultra-slow-roll, which leads to large valleys on

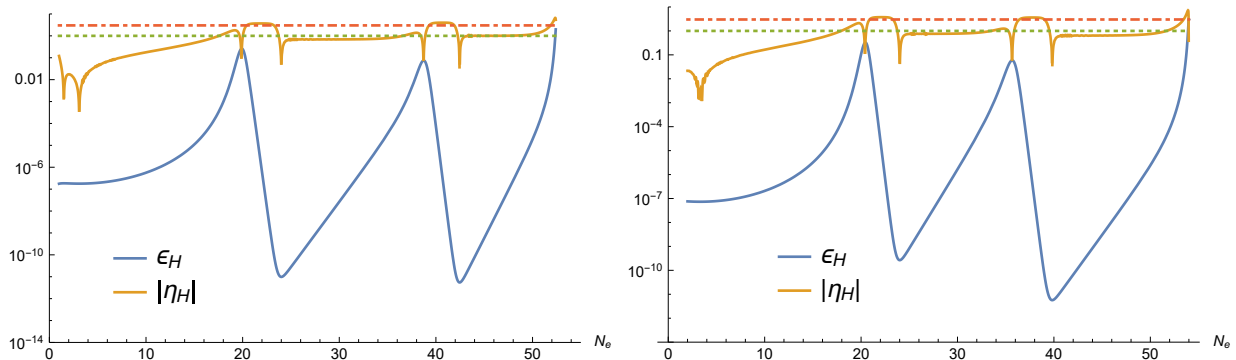


FIG. 3: Hubble slow-roll parameters ϵ_H and η_H as functions of the e-folding number N_e for Model I with parameter set (20) (left panel), Model II with parameter set (23) (right panel).

	n_s	r	$\ln(10^{10} A_s)$	N_e
Model I	0.966926	2.898×10^{-6}	3.0441	52.3
Model II	0.967783	1.182×10^{-6}	3.0444	53.9

TABLE I: The numerical results for the two models.

the curve of ϵ_H last about 15 – 20 e-folding numbers, and will give rise to double peaks in the scalar power spectrum.

The scalar spectral index as well as the tensor-to-scalar ratio can be expressed using ϵ_H and η_H as

$$\begin{aligned}
 n_s &= 1 - 4\epsilon_H + 2\eta_H, \\
 r &= 16\epsilon_H.
 \end{aligned}
 \tag{25}$$

For the two models, the numerical results of n_s and r are present in Tab.1. The amplitude of the primordial curvature perturbations A_s and the e-folding numbers during inflation N_e are also list there. The results are in agreement with the current CMB constraints $n_s = 0.9649 \pm 0.0042$, $r < 0.064$ and $\ln(10^{10} A_s) = 3.044 \pm 0.014$ from Planck 2018 [6].

Since the slow-roll approximation fails near the inflection point, the calculation of the scalar perturbations using the approximate expression $\mathcal{P}_{\mathcal{R}} \simeq \frac{1}{8\pi^2 M_P^2} \frac{H^2}{\epsilon_H}$ will underestimates

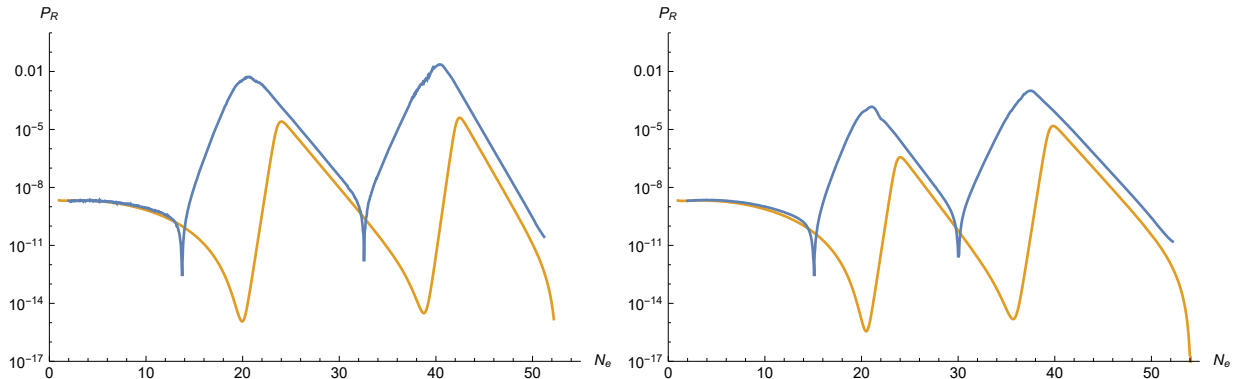


FIG. 4: Primordial power spectrum of scalar perturbations predicted by Model I with parameter set (20) (left panel), and by Model II with parameter set (23) (right panel).

the power spectrum [21, 25]. Thus it is necessary to solve the Mukhanov-Sasaki(MS) equation of mode function numerically, and then the power spectrum can be calculated by

$$\mathcal{P}_{\mathcal{R}} = \frac{k^3}{2\pi^2} \left| \frac{u_k}{z} \right|_{k \ll \mathcal{H}}^2. \quad (26)$$

The numerical results of scalar power spectrum for the two models are shown in Fig.4. The blue line is the numerical result of MS equation and the orange line is the approximate result. We can see that for both models, the scalar power spectrum matches the Planck observations at CMB scales, and has two large peaks at small scales with a height of about six to seven orders of magnitude more than the spectrum at CMB scales, such peaks will lead to the production of non-negligible second-order GWs with double peaks energy spectrum.

B. Energy spectrum of induced GWs

Using the scalar power spectrum obtained in the previous subsection, and consider that the GW energy spectrum at the present time $\Omega_{\text{GW},0}$ is related to one produced in the RD era as

$$\Omega_{\text{GW},0} = \Omega_{r,0} \left(\frac{g_{*,0}}{g_{*,p}} \right)^{1/3} \Omega_{\text{GW}}, \quad (27)$$

with $\Omega_{r,0} \simeq 9.1 \times 10^{-5}$ is the current density fraction of radiation, $g_{*,0}$ and $g_{*,p}$ are the effective degrees of freedom for energy density at the present time and at the time when the

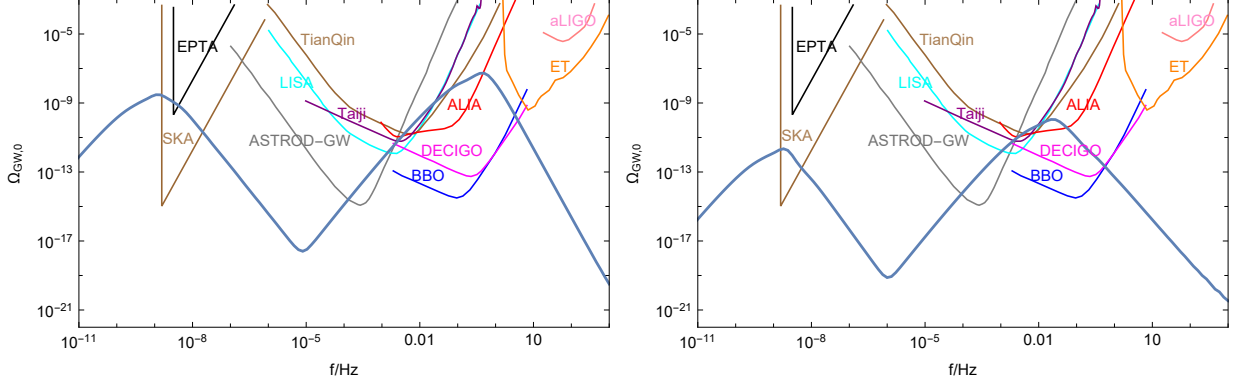


FIG. 5: Energy spectrum of the induced GWs at the present time predicted by Model I with parameter set (20) (left panel), and by Model II with parameter set (23) (right panel). The curves in the upper part are the expected sensitivity curves of the Square Kilometer Array (SKA), European Pulsar Timing Array (EPTA), Astrodynamical Space Test of Relativity using Optical-GW detector (ASTROD-GW), Taiji, Laser Interferometer Space Antenna (LISA), TianQin, Advanced Laser Interferometer Antenna (ALIA), Big Bang Observer (BBO), Deci-hertz Interferometer GW Observatory (DECIGO), Einstein Telescope (ET), Advanced LIGO (aLIGO), respectively. These sensitivity curves are taken from Ref. [24, 52–56]

peak mode crosses the horizon, respectively. We numerically calculate the energy spectrum of induced GWs for the two models and shown them as functions of the present value of the frequency f in Fig.4, with

$$f \approx 0.03\text{Hz} \frac{k}{2 \times 10^7 \text{pc}^{-1}}. \quad (28)$$

And the sensitivity curves of several planned gravitational wave detectors are also shown there [24, 52–56].

We can see that the energy spectrum of induced GWs have double peaks. The peak at low frequency, about $10^{-9} - 10^{-8} \text{Hz}$ lies above the expected sensitivity curves of SKA for both models and above EPTA for model I, and the peak at high frequency, about $0.01 - 1 \text{Hz}$ is within the frequency range of LISA [52], ALIA, Taiji [53] and TianQin [55], and the energy spectrum curves lies above the expected sensitivity curves of them. So such kind

of gravitational waves can be detected in near future. In addition, since the double peaks energy spectrum can be detected by observers in different frequency ranges thus it can be distinguish with other single peak models.

V. SUMMARY

In this paper, we investigated the possibility to induce double peaks of GW spectrum from single-field inflationary models with inflection points. We found that such double peaks spectrum can be realized by the polynomial potential from effective field theory with a cut off scale(Model I) or realized by the Higgs like ϕ^4 potential with the running of quartic coupling from radiative corrections(Model II). For some choices of parameter sets such models can give an inflationary potential with three inflection points, the inflection point at large scales can make the prediction of scalar spectral index and tensor-to-scalar ratio consistent with the current CMB constraints, and the other two inflection points can generate two large peaks in the power spectrum at small scales to induce GWs with double peaks spectrum. We calculated the energy spectrum of GWs numerically and shown that the peak at low frequency $10^{-9} - 10^{-8}Hz$, can be detected by SKA in both models or even by EPTA in Model I, and in both models, the peak at high frequency $0.01 - 1Hz$ lies above the expected sensitivity curves of LISA, ALIA, Taiji, TianQin, etc, so it can be detected in near further. In addition, since the models with double peaks energy spectrum can be detected by observers in different frequency ranges thus it can be distinguish with other single peak models.

ACKNOWLEDGMENTS

This work was supported by “the National Natural Science Foundation of China” (NNSFC) with Grant No. 11705133. XYY was supported by “the Department of edu-

cation of Liaoning province ” with Grant No.2020LNQN14.

- [1] Virgo, LIGO Scientific Collaboration, B. P. Abbott et al., Phys. Rev. Lett. 116 no. 6, (2016) 061102, arXiv:1602.03837[gr-qc].
- [2] Virgo, LIGO Scientific Collaboration, B. P. Abbott et al., Phys. Rev. Lett. 116 no. 24, (2016) 241103, arXiv:1606.04855 [gr-qc].
- [3] VIRGO, LIGO Scientific Collaboration, B. P. Abbott et al., Phys. Rev. Lett. 118 no. 22, (2017) 221101, arXiv:1706.01812 [gr-qc].
- [4] Virgo, LIGO Scientific Collaboration, B. P. Abbott et al., Phys. Rev. Lett. 119 no. 14, (2017) 141101, arXiv:1709.09660 [gr-qc].
- [5] Virgo, LIGO Scientific Collaboration, B. P. Abbott et al., Astrophys. J. 851 no. 2, (2017) L35, arXiv:1711.05578 [astro-ph.HE].
- [6] Alain Dirkes, Int. J. Mod. Phys. A Vol.33, 1830013 (2018), arXiv:1802.05958 [gr-qc]
- [7] Y. Akrami *et al.* [Planck Collaboration], arXiv:1807.06211 [astro-ph.CO].
- [8] S. Matarrese, S. Mollerach and M. Bruni, Phys. Rev. D **58**, 043504 (1998) [astro-ph/9707278].
- [9] V. Acquaviva, N. Bartolo, S. Matarrese and A. Riotto, Nucl. Phys. B **667**, 119 (2003) [astro-ph/0209156].
- [10] H. Assadullahi and D. Wands, Phys. Rev. D **79**, 083511 (2009) [arXiv:0901.0989 [astro-ph.CO]].
- [11] L. Alabidi, K. Kohri, M. Sasaki and Y. Sendouda, JCAP **1209**, 017 (2012) [arXiv:1203.4663 [astro-ph.CO]].
- [12] L. Alabidi, K. Kohri, M. Sasaki and Y. Sendouda, JCAP **1305**, 033 (2013) [arXiv:1303.4519 [astro-ph.CO]].
- [13] K. Kohri and T. Terada, Phys. Rev. D **97**, no. 12, 123532 (2018) [arXiv:1804.08577 [gr-qc]].
- [14] R. G. Cai, S. Pi and M. Sasaki, Phys. Rev. Lett. **122**, no. 20, 201101 (2019) [arXiv:1810.11000 [astro-ph.CO]].
- [15] K. Inomata and T. Nakama, Phys. Rev. D **99**, no. 4, 043511 (2019) [arXiv:1812.00674 [astro-ph.CO]].

- [16] R. G. Cai, S. Pi, S. J. Wang and X. Y. Yang, arXiv:1901.10152 [astro-ph.CO].
- [17] W. T. Xu, J. Liu, T. J. Gao and Z. K. Guo, arXiv:1907.05213 [astro-ph.CO].
- [18] J. Garcia-Bellido and E. Ruiz Morales, Phys. Dark Univ. **18**, 47 (2017) [arXiv:1702.03901 [astro-ph.CO]].
- [19] C. Germani and T. Prokopec, Phys. Dark Univ. **18**, 6-10 (2017) [arXiv:1706.04226 [astro-ph.CO]].
- [20] H. Di and Y. Gong, JCAP **1807**, no. 07, 007 (2018) [arXiv:1707.09578 [astro-ph.CO]].
- [21] Guillermo Ballesteros, Marco Taoso. Phys.Rev. D97 (2018) no.2, 023501. [arXiv:1709.05565]
- [22] I. Dalianis, A. Kehagias and G. Tringas, JCAP **1901**, 037 (2019) [arXiv:1805.09483 [astro-ph.CO]].
- [23] J. M. Ezquiaga, J. Garcia-Bellido and E. Ruiz Morales, Phys. Lett. B **776**, 345-349 (2018) [arXiv:1705.04861 [astro-ph.CO]].
- [24] M. Drees and Y. Xu, arXiv:1905.13581 [hep-ph].
- [25] T. J. Gao and Z. K. Guo, Phys. Rev. D **98**, no. 6, 063526 (2018) [arXiv:1806.09320 [hep-ph]].
- [26] M. Kawasaki, A. Kusenko, Y. Tada and T. T. Yanagida, Phys. Rev. D **94**, no.8, 083523 (2016) [arXiv:1606.07631 [astro-ph.CO]].
- [27] O. Özsoy, S. Parameswaran, G. Tasinato and I. Zavala, JCAP **07**, 005 (2018) [arXiv:1803.07626 [hep-th]].
- [28] T. J. Gao and X. Y. Yang, Int. J. Mod. Phys. A **34**, no.32, 1950213 (2019)
- [29] M. Cicoli, V. A. Diaz and F. G. Pedro, JCAP **06**, 034 (2018) doi:10.1088/1475-7516/2018/06/034 [arXiv:1803.02837 [hep-th]].
- [30] J. Liu, Z. K. Guo and R. G. Cai, Phys. Rev. D **101**, no.8, 083535 (2020) [arXiv:2003.02075 [astro-ph.CO]].
- [31] D. Baumann, P. J. Steinhardt, K. Takahashi and K. Ichiki, Phys. Rev. D **76**, 084019 (2007) [hep-th/0703290].
- [32] K. N. Ananda, C. Clarkson and D. Wands, Phys. Rev. D **75**, 123518 (2007) [gr-qc/0612013].
- [33] K. Ando, K. Inomata, M. Kawasaki, K. Mukaida and T. T. Yanagida, Phys. Rev. D **97** (2018) no.12, 123512 [arXiv:1711.08956 [astro-ph.CO]].
- [34] H. Kodama and M. Sasaki, Prog. Theor. Phys. Suppl. **78**, 1 (1984).

- [35] V. F. Mukhanov, H. A. Feldman and R. H. Brandenberger, Phys. Rept. **215**, 203 (1992).
- [36] J. R. Espinosa, D. Racco, and A. Riotto JCAP 09 (2018) 012 [arXiv:1804.07732 [hep-ph]].
- [37] N. Bhaumik and R. K. Jain, JCAP **01**, 037 (2020) [arXiv:1907.04125 [astro-ph.CO]].
- [38] K. Enqvist and A. Mazumdar, Phys. Rept. **380**, 99-234 (2003) [arXiv:hep-ph/0209244 [hep-ph]].
- [39] C. P. Burgess, H. M. Lee and M. Trott, JHEP **09**, 103 (2009) [arXiv:0902.4465 [hep-ph]].
- [40] F. Marchesano, G. Shiu and A. M. Uranga, JHEP **09**, 184 (2014) [arXiv:1404.3040 [hep-th]].
- [41] M. P. Hertzberg, M. Yamada Phys. Rev. D 97, 083509 (2018) [arXiv:1712.09750 [astro-ph.CO]]
- [42] G. Ballesteros, J. Rey, M. Taoso and A. Urbano JCAP 07 (2020) 025 [arXiv:2001.08220 [astro-ph.CO]]
- [43] G. Ballesteros and C. Tamarit, JHEP **02**, 153 (2016) doi:10.1007/JHEP02(2016)153 [arXiv:1510.05669 [hep-ph]].
- [44] Sidney R. Coleman and Erick J. Weinberg. Radiative Corrections as the Origin of Spontaneous Symmetry Breaking. Phys.Rev., D7:1888C1910, 1973.
- [45] C. Germani and T. Prokopec, Phys. Dark Univ. **18**, 6 (2017) [arXiv:1706.04226 [astro-ph.CO]].
- [46] K. Dimopoulos, Phys. Lett. B **775**, 262 (2017) [arXiv:1707.05644 [hep-ph]].
- [47] J. M. Ezquiaga and J. Garca-Bellido, JCAP 1808 (2018) 018, [arXiv:1805.06731 [astro-ph]].
- [48] D. Cruces, C. Germani and T. Prokopec, JCAP 1903 (2019) no.03, 048 , [arXiv:1807.09057 [gr-qc]].
- [49] D. J. Schwarz, C. A. Terrero-Escalante and A. A. Garcia, Phys. Lett. B **517**, 243 (2001) [astro-ph/0106020].
- [50] S. M. Leach, A. R. Liddle, J. Martin and D. J. Schwarz, Phys. Rev. D **66**, 023515 (2002) [astro-ph/0202094].
- [51] D. J. Schwarz and C. A. Terrero-Escalante, JCAP **0408**, 003 (2004) [hep-ph/0403129].
- [52] H. Audley et al. [arxiv:1702.00786 [astro-ph.IM]].
- [53] Z. K. Guo, R. G. Cai and Y. Z. Zhang, arXiv:1807.09495 [gr-qc].
- [54] C. J. Moore, R. H. Cole and C. P. L. Berry, Class. Quant. Grav. 32 (2015) no.1, 015014, [arXiv:1408.0740 [gr-qc]].

- [55] J. Luo et al. [TianQin Collaboration], *Class. Quant. Grav.* **33** (2016) no.3, 035010, [arXiv:1512.02076 [astro-ph.IM]].
- [56] K. Kuroda, W. T. Ni and W. P. Pan, *Int. J. Mod. Phys. D* **24** (2015) no.14, 1530031, [arXiv:1511.00231 [gr-qc]].